MS-TP-18-04
DESY 18-008

The light bound states of $\mathcal{N} = 1$ supersymmetric SU(3) Yang-Mills theory on the lattice

Sajid Ali*[1], Georg Bergner†[2,1], Henning Gerber*[1], Pietro Giudice*[1], Istvan Montvay‡[3], Gernot Münster*[1], Stefano Piemonte§[4], and Philipp Scior*[1]

[1]University of Münster, Institute for Theoretical Physics, Wilhelm-Klemm-Str. 9, D-48149 Münster, Germany
[2]University of Jena, Institute for Theoretical Physics, Max-Wien-Platz 1, D-07743 Jena, Germany
[3]Deutsches Elektronen-Synchrotron DESY, Notkestr. 85, D-22607 Hamburg, Germany
[4]University of Regensburg, Institute for Theoretical Physics, Universitätsstr. 31, D-93040 Regensburg, Germany

January 24, 2018

In this article we summarise our results from numerical simulations of $\mathcal{N} = 1$ supersymmetric Yang-Mills theory with gauge group SU(3). We use the formulation of Curci and Veneziano with clover-improved Wilson fermions. The masses of various bound states have been obtained at different values of the gluino mass and gauge coupling. Extrapolations to the limit of vanishing gluino mass indicate that the bound states form mass-degenerate supermultiplets.

*{sajid.ali,h.gerber,p.giudice,munsteg,scior}@uni-muenster.de
†georg.bergner@uni-jena.de
‡montvay@mail.desy.de
§stefano.piemonte@ur.de

1. Introduction

Supersymmetric gauge theories are building blocks for many extensions of the Standard Model that aim to describe the physics of fundamental interactions beyond the TeV scale. In general, the non-perturbative properties of these theories play an essential role, in particular concerning the scenarios for a dynamical supersymmetry (SUSY) breaking. Monte-Carlo simulations on the lattice are the method of choice for non-perturbative investigations of quantum field theories. They provide a tool to investigate if and how the theoretical predictions about supersymmetric theories are realised, see [1] for a more general discussion.

A specific application of numerical simulations of supersymmetric theories is the determination of the spectrum of bound states and the study of the gluino condensate in $\mathcal{N} = 1$ supersymmetric Yang-Mills theory (SYM). In fact, scenarios have been proposed for the multiplet structure of the lightest bound states of this theory [2, 3, 4], and several analytical calculations have been presented for the chiral condensate, see [5] and references therein. The bound state spectrum is the main focus of our current investigations. In our previous project we have mainly considered SYM with gauge group SU(2). We have investigated the particle spectrum of the theory and observed the expected degeneracy of the states in the lightest supermultiplet [6]. We have now extended our studies to the multiplet of excited states, and first results have been reported in a contribution to the Lattice2017 conference [7].

Our most recent efforts are the numerical simulations of $\mathcal{N} = 1$ supersymmetric Yang-Mills theory with gauge group SU(3). This theory is more appealing from a phenomenological point of view, since it corresponds to the gauge part of supersymmetric QCD. First results for this theory by our collaboration can be found in [8, 9, 10]. Another investigation of this theory is presented in [11]. Our simulations rely on the specific approach of using Wilson fermions and a tuning of the gluino mass to restore chiral symmetry and supersymmetry. As has been found by Veneziano and Curci, this tuning is enough to recover both symmetries in the continuum limit [12]. We crosscheck the correctness of our tuning using the supersymmetric Ward identities.

Simulations of theories with dynamical fermions in the adjoint representation of SU(3), such as SYM, require significantly more resources than QCD with quarks in the fundamental representation. Therefore, at present we are bound to relatively small lattice sizes. The removal of the leading order lattice cut-off terms from the fermion action is crucial in this case, since lattice artefacts lead to an explicit supersymmetry breaking. From our previous investigations we have found that the clover improved fermion action is definitively a better choice than the unimproved stout smeared Wilson fermions used in our first simulations [9]. Further details of our lattice formulation are explained in Section 2.

The main focus of our project are the investigations of the lightest bound states masses in SU(3) SYM. In particular, we want to check whether the mass degeneracy between bosonic and fermionic particles expected in a supersymmetric theory is realised non-perturbatively in the spectrum of bound states. Analytic calculations based on low-energy effective actions predict a supermultiplet of bound states consisting of mesonic

gluinoballs and fermionic gluino-glue particles [2]. It was later extended by an additional multiplet containg states created by glueball operators [3, 4]. We investigate the members of both multiplets on the lattice by means of suitable operators. The results at one value of the lattice spacing, presented in Section 5, already indicate the expected formation of the supermultiplets of the lowest-lying states as in the case of gauge group SU(2).

In Section 3 the methods for the determination of the dimensionful reference scales are explained. Issues concerning the systematic errors, like the check for an efficient sampling of topological sectors, are discussed in Section 6. Finally, as an outlook we provide first results at three additional lattice spacings in Section 7.

2. The improved lattice formulation of supersymmetric Yang-Mills theory

Supersymmetric SU(3) Yang-Mills theory describes gluons, the particles associated with the non-Abelian gauge field for gauge group SU(3), and their superpartners, the gluinos. Gluinos are Majorana fermions transforming under the adjoint (octet) representation of SU(3). SU(3) SYM is of a complexity comparable to QCD [13]. It is expected that in the continuum the particles described by this theory are bound states of gluons and gluinos, that form supermultiplets degenerate in their masses, if supersymmetry is unbroken. Since supersymmetry is broken explicitly by the lattice discretisation, one important task of the project is to demonstrate that the data of the numerical simulations are consistent with restoration of supersymmetry in the continuum limit.

In the continuum the (on-shell) Lagrangian of SYM, containing the gluon fields A_μ and the gluino field λ, reads

$$\mathcal{L} = \mathrm{tr}\left[-\frac{1}{2}F_{\mu\nu}F^{\mu\nu} + \mathrm{i}\,\bar{\lambda}\gamma^\mu D_\mu\lambda - m_0\bar{\lambda}\lambda\right], \tag{1}$$

where $F_{\mu\nu}$ is the non-Abelian field strength and D_μ denotes the gauge covariant derivative in the adjoint representation. The gluino mass term with the bare mass parameter m_0 breaks supersymmetry softly.

We employ the lattice formulation of SYM proposed by Curci and Veneziano [12]. The gauge field is represented by link variables $U_\mu(x)$. The corresponding gauge action is the Wilson action built from the plaquette variables U_p. The gluinos are described by Wilson fermions in the adjoint representation. In its basic form the lattice action reads

$$\mathcal{S}_L = \beta\sum_p\left(1 - \frac{1}{3}\mathrm{Re}\,\mathrm{tr}\,U_p\right) + \frac{1}{2}\sum_{xy}\bar{\lambda}_x(D_w)_{xy}\lambda_y\,, \tag{2}$$

with the Wilson-Dirac operator

$$\begin{aligned}(D_w)_{x,a,\alpha;y,b,\beta} &= \delta_{xy}\delta_{a,b}\delta_{\alpha,\beta} - \kappa\sum_{\mu=1}^{4}\left[(1-\gamma_\mu)_{\alpha,\beta}(V_\mu(x))_{ab}\delta_{x+\mu,y}\right.\\ &\quad\left.+(1+\gamma_\mu)_{\alpha,\beta}(V_\mu^\dagger(x-\mu))_{ab}\delta_{x-\mu,y}\right],\end{aligned} \tag{3}$$

where $V_\mu(x)$ are the link variables in the adjoint representation. The hopping parameter κ is related to the bare gluino mass via $\kappa = 1/(2m_0 + 8)$.

In our current simulations we have implemented the clover term in order to reduce the leading lattice artefacts of the Wilson fermion action. The additional term is

$$-\frac{c_{sw}}{4}\,\bar{\lambda}(x)\sigma_{\mu\nu}F^{\mu\nu}\lambda(x). \tag{4}$$

where $F_{\mu\nu}$ is the clover plaquette. We have used the one-loop value for the coefficient c_{sw} [14], leading to a one-loop $O(a)$ improved lattice action. This is a systematic and feasible approach for setting the clover coefficient. Alternative tunings of the coefficient are possible. In the SU(2) case we have tested a tadpole resummation [6], that leads to a considerable improvement of the mass degeneracy for finite lattice spacings. At our current parameter range the value of c_{sw} obtained with the proposed tadpole formula is not much different from the one-loop prediction.

The integration of the Majorana fermions yields

$$\int [d\lambda]\ \mathrm{e}^{-\frac{1}{2}\bar{\lambda}D_w\lambda} = \mathrm{Pf}(CD_w) = \pm\sqrt{\det D_w} \tag{5}$$

which is the Pfaffian of the Wilson-Dirac operator D_w multiplied with the charge conjugation matrix C. The square root of the determinant is handled by the RHMC algorithm, whereas the sign of the Pfaffian has to be considered in a reweighting of the observables. The effect of the Pfaffian sign is discussed in Section 6.1.

3. Scale setting and simulation parameters

We have performed simulations at four different values of the inverse gauge coupling $\beta = 5.4$, 5.5, 5.6, and 5.8. The lattice size is $16^3 \times 32$, except for $\beta = 5.4$, where we have chosen a $12^3 \times 24$ lattice, and some additional large volume runs at $\beta = 5.6$. The most reliable results are obtained at $\beta = 5.5$, whereas especially the results at $\beta = 5.8$ are in most cases excluded due to considerable finite size effects, as discussed in detail in Section 6.

The scale is determined from an independent measurement of gluonic observables in order to estimate the lattice spacing and the physical volume. We are using two different quantities: the Sommer parameter r_0 and the scale w_0 from the gradient flow [15, 16]. The results in units of r_0 can be converted to QCD units fm or MeV using the QCD scale setting $r_0 = 0.5\,\mathrm{fm}$. The methods for the determination of r_0/a from a fit of the static quark-antiquark potential are explained in our earlier work on SU(2) SYM [6]. At each β the final values of the scales w_0/a and r_0/a are obtained by linearly extrapolating them as a function of the square of the adjoint pion mass to the chiral limit.

The determination of w_0/a follows the standard methods [15, 16] up to a modification of the reference point. We have chosen a reference value of $u = 0.2$ ($w_0^{0.2}$) instead of the common value 0.3 ($w_0^{0.3}$). This method is explained in [17] and reduces the effect of topological freezing that we observe at our smallest lattice spacings. The scaling between

$\beta = 5.4$ and $\beta = 5.5$ is compatible for $w_0^{0.2}/a$ and $w_0^{0.3}/a$. Up to $\beta = 5.6$ the scaling of $w_0^{0.2}$ is consistent with the r_0 scaling. The smaller value of u also considerably reduces the quite large uncertainties for the chiral extrapolation of w_0 at $\beta = 5.6$.

4. Signals for supersymmetry and chiral symmetry restoration

As shown by Veneziano and Curci [12], supersymmetry and chiral symmetry are restored in the continuum limit by the same tuning of the bare gluino mass m_0. Chiral symmetry restoration cannot be probed directly from the chiral Ward identities as in the case of two-flavour QCD, since the U(1) axial symmetry is broken explicitly by an anomaly and not only by the Wilson term. An alternative way is provided by the mass of the adjoint pion (a–π). The adjoint pion is not a physical particle in SYM. It can, however, be defined by arguments based on the OZI-approximation [2], or in the framework of partially quenched chiral perturbation theory [18]. When SYM is considered as the partially quenched limit of Yang-Mills theory with two Majorana flavours, the adjoint pion can be interpreted as a pseudo-Nambu-Goldstone particle arising from spontaneous chiral symmetry breaking. In the presence of an explicit chiral symmetry breaking by a non-vanishing renormalised gluino mass, the square of the adjoint pion mass scales proportional to the renormalised gluino mass. This relation is used to extrapolate our numerical results to the chiral limit. The mass of the adjoint pion (m_π) is measured from the exponential decay of the connected part of the a–η' meson correlator.

The reliability of our approach for the tuning to the chiral-supersymmetric continuum limit has to be crosschecked with different prescriptions. Supersymmetric Ward identities provide an alternative solid signal for the remnant chiral symmetry breaking without further assumptions about the structure of chiral effective actions. Another approach is to determine the transition point for the discrete subgroup of chiral symmetry that is left unbroken by the anomaly. Below we discuss in detail the theoretical expectations and the results of these different tunings towards the chiral limit. All of these signals must agree in the continuum limit, but we will show that already at finite lattice spacings the discrepancies are small and even negligible compared to other systematic uncertainties.

We have investigated the supersymmetric Ward identities at many different values of our bare mass parameter. A combination of the supercurrent renormalisation constant (Z_S) and the renormalised gluino mass (m_S) can be determined from this measurement. The techniques of the measurement and analysis can be found in [19, 20]. We developed a generalised least squares method [21, 20] to obtain more reliable estimates of $am_S Z_S^{-1}$ and its statistical error. Note that the tuning of the clover coefficient in the fermion action up to one-loop order does not ensure automatically the $O(a)$ improvements of the SUSY Ward identities, as explained in [19]. Further perturbative calculations of improvement coefficients would be required to reach an $O(a)$ scaling of the same order, and we plan to investigate this aspect in the future.

The value of the critical parameter κ_c, where the renormalised gluino mass vanishes, is

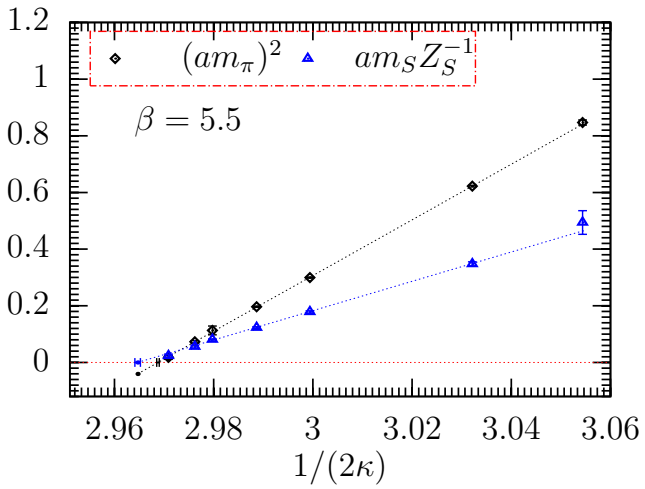

Figure 1: Linear extrapolations of the adjoint pion mass squared (m_π^2) (black) and the renormalised gluino mass ($am_S Z_S^{-1}$) obtained by SUSY Ward identities (blue) as a function of the bare parameter κ towards the chiral point (κ_c).

obtained from an extrapolation of m_π^2 to zero, and it is compared with the determination from the supersymmetric Ward identities, as shown in Figure 1. The two values of κ_c are very close to each other, but there is a small difference of around 0.00023(5). This discrepancy is presumably due to lattice artifacts, and is expected to disappear in the continuum limit. Results at other values of β in view of the continuum limit are discussed in [20].

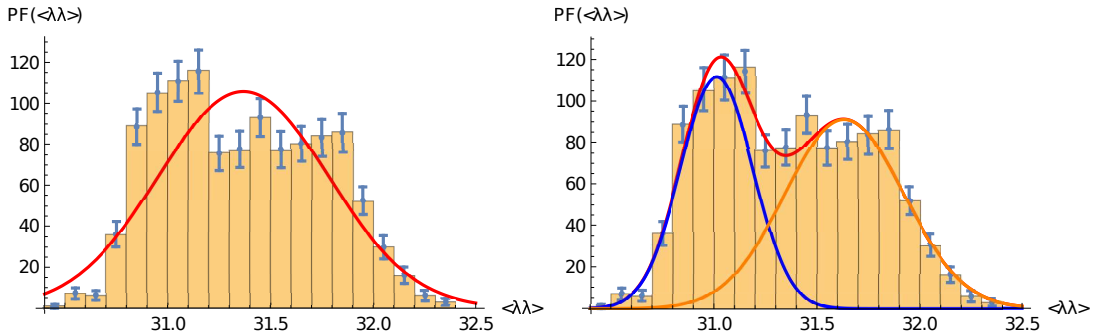

(a) Single Gaussian fit

(b) Double Gaussian fit

Figure 2: Double peak structure of the histogram of the chiral condensate at $\kappa = 0.1665$ and $\beta = 5.6$ from 1200 configurations. A single Gaussian does not fit our data, which are instead consistent with a sum of two Gaussian functions.

A third determination of κ_c could be found by studying the change of the gluino condensate at zero temperature occurring at the chiral phase transition. In fact, chiral

symmetry is the invariance of the continuum action of SYM with respect to the U(1) rotation of the fermion field

$$\lambda \to \exp\{-\mathrm{i}\theta\gamma_5\}\lambda\,. \tag{6}$$

An anomaly breaks chiral symmetry down to Z_{2Nc} at the quantum level, such that only $2N_c$ values of θ leave the partition function invariant. At zero temperature even the discrete group Z_{2Nc} is broken down spontaneously to Z_2 by a non-vanishing expectation value of the gluino condensate. The coexistence of N_c degenerate vacua is a signal for a first order phase transition crossing the chiral limit as a function of the gluino mass. We can search the transition in the chiral condensate $\langle\bar{\lambda}\lambda\rangle$, corresponding to the real part of the gluino condensate. The condensate on each configuration should hence fluctuate between two distinct values at the critical point κ_c. However, simulations close to the critical point are very difficult and we are limited to small volumes, like 6^4 and 8^4, to ensure the convergence of the inverter of the Dirac-Wilson operator. We have used periodic boundary conditions to reduce the breaking of supersymmetry that would otherwise appear at non-zero temperature due to the difference between the thermal statistics of fermions and bosons. Running our simulations at $\beta = 5.6$, we find signals of a double-peak structure of the chiral condensate at $\kappa = 0.1665$, see Figure 2. The determined value of κ_c is consistent with the other determinations ($\kappa_c(m_\pi) = 0.16635(4)$, $\kappa_c(\langle\bar{\lambda}\lambda\rangle) = 0.1662(4)$). Taking into account the uncertainties from finite size effects, we can conclude that there is a good agreement with the theoretical expectations concerning the vacuum structure of the theory at zero temperature.

5. Results for the lightest supermultiplet in supersymmetric SU(3) Yang-Mills theory

The estimation of the masses of bound states in SU(3) SYM is the main focus of the current work. The particle spectrum is composed of bound states of gluons and gluinos. One expects composites of gluino fields (gluinoballs), of gluon fields (glueballs), and of both (gluino-glueballs). The physical states would be mixtures of those. The measurement of these particles is quite challenging. For the mesonic gluinoballs, which are flavour singlet mesons, and the glueballs this can be understood by comparison with the corresponding particles in QCD. Hence a rather large statistics is required in order to get reliable estimates for the masses. As detailed in Section 4, the adjoint pion mass is used for the extrapolations of the masses to the chiral limit. All masses are determined from the exponential decay of the correlators in the corresponding channels. Further details of the different measurements are explained in the following. First we consider the simulations at $\beta = 5.5$ on a $16^3 \times 32$ lattice, since these are our most precise and most reliable results.

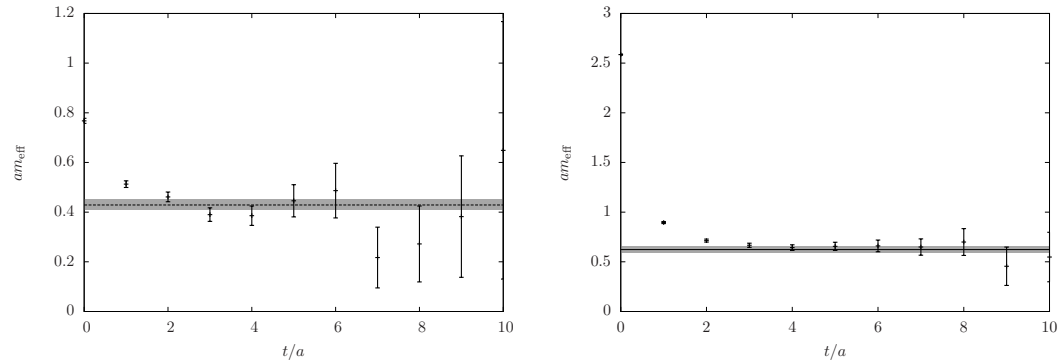

(a) Glueball (b) Gluino-glue

Figure 3: Mass plateau of the gluino-glue and the 0^{++} glueball for $\beta = 5.5$, $\kappa = 0.1673$, on a $16^3 \times 32$ lattice. The final value indicated by the gray line is obtained from a fit of the correlation function.

5.1. Glueballs, gluino-glueballs and the supermultiplet formation

A reliable determination of the glueball masses is challenging. In the current work we have focused on the 0^{++} glueball, since it provides the best signal-to-noise ratio. We have applied variational methods to reduce the effects of excited states. More about our methods is explained in our work on SU(2) SYM [6] and in [22]. An example of an effective mass determined from the exponential decay of the correlators is shown in Figure 3(a).

The fermionic partners of the glueballs are particles created from gluino and gluon fields. The corresponding operator is composed of the field strength $F_{\mu\nu}$ and the gluino field,

$$\tilde{O}_{g\tilde{g}} = \sum_{\mu\nu} \sigma_{\mu\nu} \mathrm{Tr}\left[F^{\mu\nu}\lambda\right], \tag{7}$$

with $\sigma_{\mu\nu} = \frac{1}{2}[\gamma_\mu, \gamma_\nu]$. $F_{\mu\nu}$ is represented by the clover plaquette on the lattice. The measurement of this particle from the ensemble of gauge configurations uses Jacobi and APE smearing techniques in order to improve the signal and to suppress the excited state contaminations. Figure 3(b) shows an example of the effective mass and of the quality of our fits. Further details can be found in our earlier publications [6].

As in our previous investigations of SU(2) SYM, the degeneracy of the fermionic gluino-glue and its bosonic partners is the most important signal for the supermultiplet formation. The chiral extrapolation of the 0^{++} glueball and gluino-glue masses at $\beta = 5.5$ are shown in Figure 4. At large adjoint pion masses, corresponding to a large soft supersymmetry breaking, the gluino-glue is about twice as heavy as the glueball. However, in the chiral limit the two masses become degenerate up to our current statistical precision.

In general, supersymmetry breaking lattice artefacts, indicated by a mass gap between the states of the lightest supermultiplet, are expected at any finite lattice spacing. In our current simulations at $\beta = 5.5$ their influence seems to be under control since the

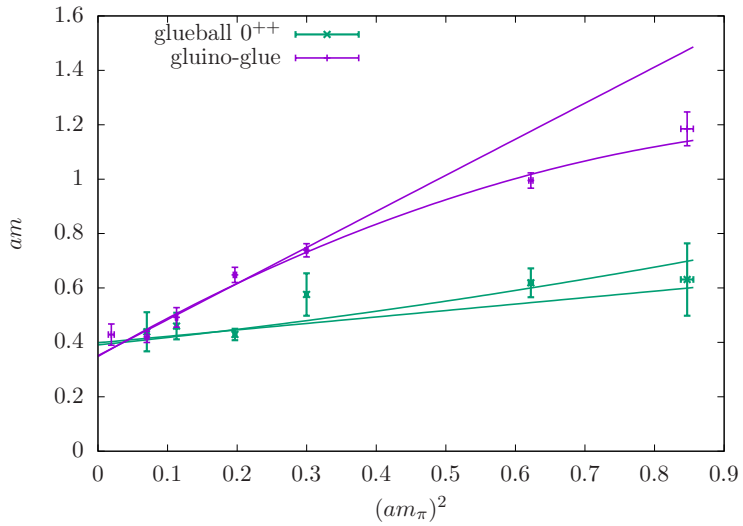

Figure 4: The masses of the gluino-glue and the 0^{++} glueball at $\beta = 5.5$ in lattice units. The figure shows a linear and a quadratic fit of the data. The two largest values of the adjoint pion mass m_π are excluded in the linear fit of the gluino-glue.

mass gap is not significantly larger than other uncertainties of the measurements. At these parameters our simulations therefore are already close enough to the continuum limit to reproduce main features of the continuum theory.

5.2. The completion of the chiral multiplet by mesonic gluinoballs

Two chiral supermultiplets are expected to represent the degrees of freedom at low energies. The supermultiplet of the lightest bound states should contain a scalar, a pseudoscalar, and a fermionic particle. The scalar and pseudoscalar particles described by the low-energy effective actions are either of glueball or of mesonic type. The actual states would, however, be mixtures of those, and on the lattice the states created by the corresponding glueball and mesonic operators cannot be distinguished unambiguously.

In our previous investigation of SU(2) SYM we have found that the mesonic operator provides a better signal for the lightest pseudoscalar state, whereas the scalar meson is degenerate with the scalar glueball. We complete the results for the masses of the lowest multiplet with the additional data from the a–η' meson for the pseudoscalar channel and use the a–f_0 as a cross check for the scalar glueball data.

The singlet mesonic operators are named similar to their QCD counterparts, the pseudoscalar a–η' ($\bar{\lambda}\gamma_5\lambda$) and the scalar a–$f_0$ ($\bar{\lambda}\lambda$). The disconnected part is an essential contribution to the correlation functions of these particles. The signal for this part of the correlators is rather noisy. Our methods for the measurement include truncated eigenmode approximation and preconditioning to improve the signal, see [23] for further details. The results contain still quite large uncertainties, see Figure 5, but we are able to obtain the first estimates of the masses also in the mesonic channel. We have also

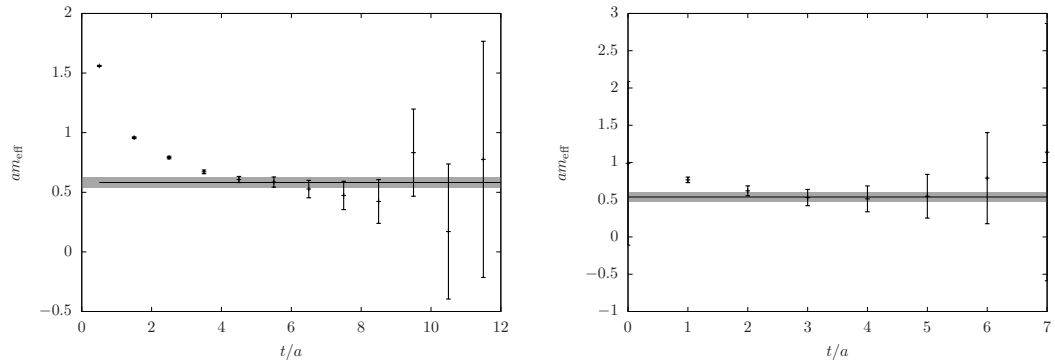

(a) a–η' (b) a–f_0

Figure 5: Mass plateau for the mesons a–η' and a–f_0 for $\beta = 5.5$, $\kappa = 0.1673$, on a $16^3 \times 32$ lattice. The final value indicated by the gray line is obtained from a fit of the correlation function.

done an alternative determination of the a–η' mass from the topological charge density correlator [24], which is in good agreement with the results obtained from the mesonic correlators.

The signal in the scalar and pseudoscalar channels can be improved using a variational approach combining different mesonic and gluonic operators. We have recently tested this in SU(2) SYM [7], and we plan to use it also in the SU(3) case. Most likely it will reduce the remnant excited state contamination of the ground state signal, especially in the mesonic sector.

As shown in Figure 6, the masses of the scalar and pseudoscalar mesons are almost degenerate with the scalar glueball mass within our current precision. Similar to the scalar glueball, they show only a weak fermion mass dependence. There is indeed a formation of a complete supersymmetry multiplet in the chiral limit and the a–f_0 provides a signal for the same lightest scalar state as the glueball.

The final extrapolated values of the particle masses in units of the Sommer scale r_0 are

gluino-glue	glueball 0^{++}	a–η'	a–f_0
2.83(44)	3.22(95)	3.70(71)	3.69(63)

6. Estimation of systematic uncertainties

Several systematic uncertainties of our current results need to be considered. The most important limitation is the remnant supersymmetry breaking by the lattice discretisation. We are currently not able to perform a complete extrapolation to the continuum, but as explained in Section 7, the remaining uncertainties are currently at the order of the statistical errors. We plan more in-depth investigations to get a better signal for the continuum extrapolation. The finest accessible lattice spacing is limited by two effects. Since the number of lattice points is limited, the finer lattice spacing leads to a smaller

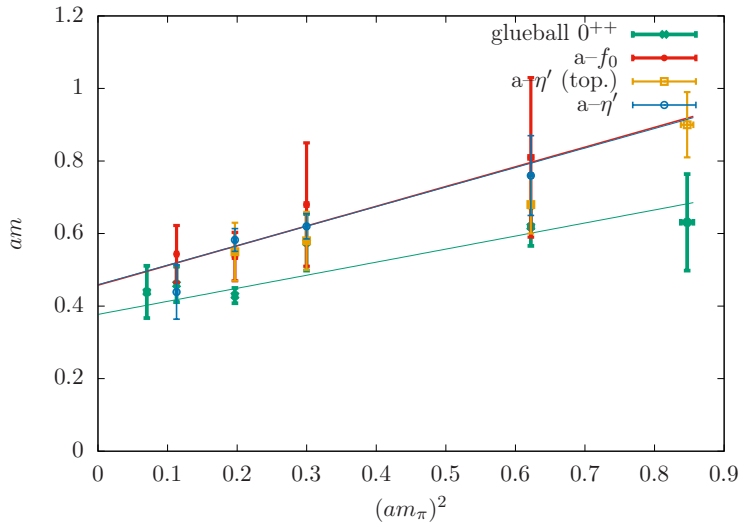

Figure 6: The masses of the different bosonic particles (singlet scalar and pseudoscalar mesons) in comparison to the glueball mass at $\beta = 5.5$. a–η'(top.) indicates the pseudoscalar meson mass obtained from the topological charge density correlator.

volume. The lattice spacing can, consequently, only be reduced until the finite volume effects significantly affect the results. The second important effect is the topological freezing, that leads to large autocorrelation times when the lattice spacing becomes too small. As we will discuss below, our simulations at $\beta = 5.6$ and $\beta = 5.8$ are affected by these effects.

6.1. The Pfaffian sign

The sign of the Pfaffian has to be taken into account in our simulations. We expect that the Pfaffian sign is not significant at our current parameters, but this has to be confirmed by measurements. The fluctuations of the Pfaffian sign become more significant at smaller gluino masses and coarser lattices. It is hence possible to approach the chiral continuum limit from simulations without a relevant contribution of the sign. However, we have to check explicitly that we are indeed in the region without relevant negative sign contributions. It is enough to consider the run with the smallest gluino mass to confirm this. As explained in our earlier investigations, the sign of the Pfaffian is obtained from the number of degenerate pairs of real negative eigenvalues of the Dirac-Wilson operator, see also [25] for the methods of this measurement. Sign changes are hence only possible, if there are negative real eigenvalues. As shown in Figure 7 we do not observe any of these negative eigenvalues at least for a large subset of configurations. We conclude that the Pfaffian sign for the current runs at $\beta = 5.5$ is not relevant.

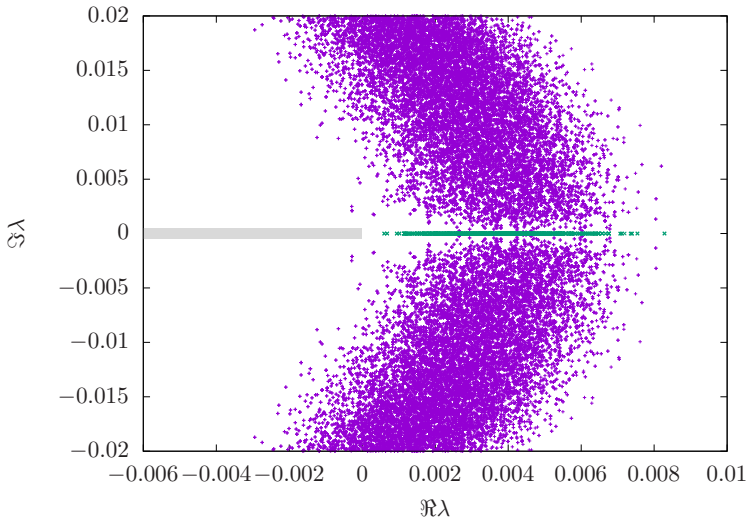

Figure 7: The eigenvalues of the Dirac-Wilson operator in the complex plane, relevant for the sign of the Pfaffian, from 1022 configurations at $\beta = 5.5$, $\kappa = 0.1683$. The green points indicate eigenvalues with a significant chirality of the eigenvector $\langle v|\gamma_5|v\rangle > 0.001$. Possible Pfaffian sign changes might occur if there are real negative eigenvalues, i. e. green points in the shaded region.

6.2. Finite size effects

Finite size effects play an important role in the estimations of the mass spectrum. In earlier investigations with gauge group SU(2) we have found that for small volumes the gluino-glue gets heavier and the degeneracy of the spectrum is lost, but larger volumes ($L/r_0 > 2.4$) are not affected [26]. We check whether similar finite volume effects also appear for gauge group SU(3) at a rather small lattice spacing ($\beta = 5.6$). The results shown in Figure 8 have a considerable uncertainty for the gluino-glue data. At the lattice size of $N_s = 16$, where we have performed most of the simulations, the adjoint pion mass shows around 10% finite size effects. We conclude that on a $16^3 \times 32$ lattice the finite size effects are negligible at $\beta = 5.5$; at $\beta = 5.6$ they are of the order of our current still quite limited accuracy. At $\beta = 5.8$ rather large finite size effects are expected. Consequently we have focussed here on $\beta = 5.5$ and plan to increase the lattice volume in our future more precise simulations at $\beta = 5.6$.

6.3. The sampling of topological sectors

As known from QCD, topological sectors are not efficiently sampled at lattice spacings smaller than roughly 0.05 fm, leading to the loss of ergodicity of Monte-Carlo lattice simulations. Very large autocorrelation times are especially observed for topological quantities, and the topological charge is effectively frozen towards the continuum limit. Our simulations are already at a very fine lattice spacing, therefore we must ensure a reasonable sampling of the topological sectors. We have measured the average topological

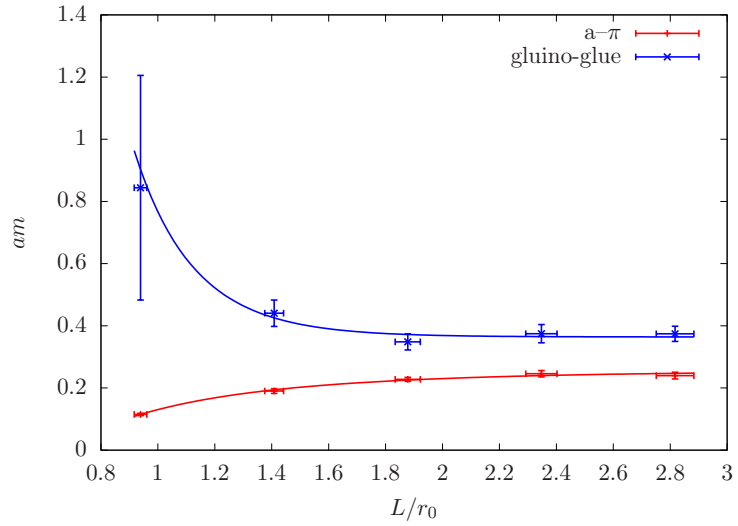

Figure 8: The adjoint pion and gluino-glue mass from simulations at $\beta = 5.6$, $\kappa = 0.1660$ on lattices of size $8^3 \times 32$, $12^3 \times 32$, $16^3 \times 32$, $20^3 \times 40$, and $24^3 \times 48$. These data indicate the magnitude of finite size effects. The results have been fitted assuming a finite size correction proportional to $\exp(-\alpha L)/L$ with some positive coefficient α.

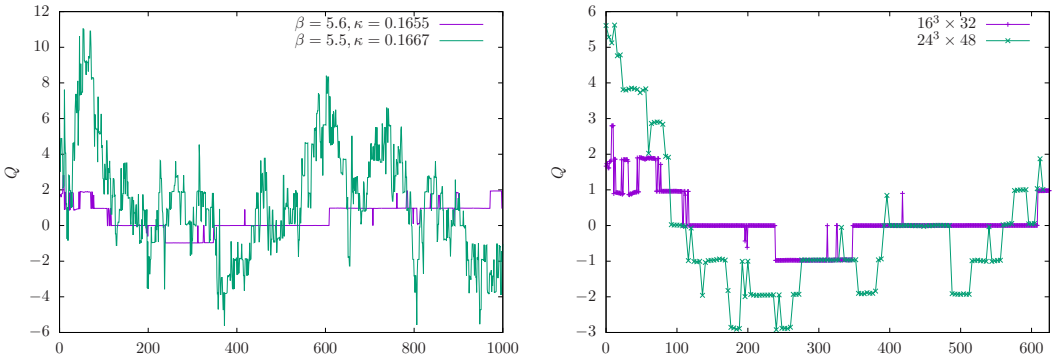

(a) β dependence (b) volume dependence

Figure 9: Left hand side: The history of the topological charge from simulations at $\beta = 5.5$ and $\beta = 5.6$ on a $16^3 \times 32$ lattice. Right hand side: The history of the topological charge at $\beta = 5.6$, $\kappa = 0.1660$ for two different volumes.

charge $\langle Q \rangle$, the corresponding integrated autocorrelation time τ_Q, and the topological susceptibility χ_Q. The topological freezing is under control for $\beta = 5.5$ (τ_Q is between 17 and 46), but starts to become more significant at $\beta = 5.6$ (τ_Q is between 58 and 185), which might also be related to the small volume, see Figure 9. The histogram of the topological charge for $\beta = 5.8$ shows a nearly frozen topology. Hence, for this β the values of τ_Q and other quantities are not reliable.

7. Outlook: continuum limit and comparison to the SU(2) case

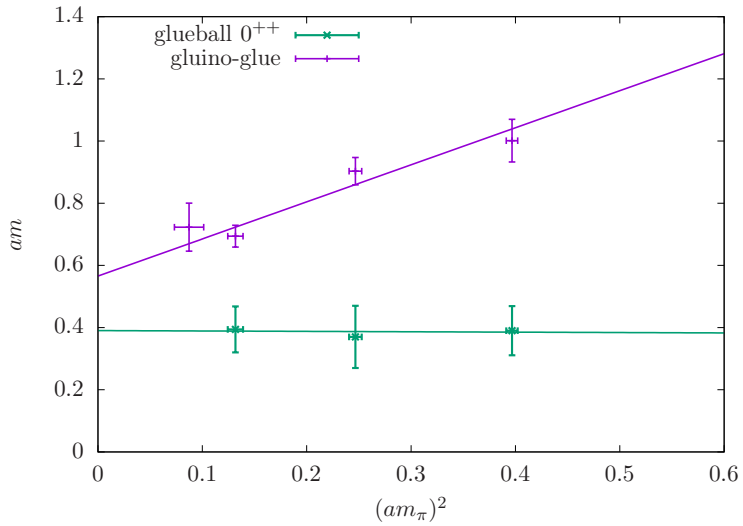

Figure 10: The masses of the fermionic gluino-glue and the bosonic 0^{++} glueball at $\beta = 5.4$ in lattice units. The figure includes an extrapolation of the chiral limit based on a linear fit.

Currently our most precise results are from $\beta = 5.5$. The results from the finer lattices are limited by finite size effects and topological freezing. In addition we have done simulations at one coarser lattice at $\beta = 5.4$. Our first preliminary results for the glueball and the gluino-glue at the coarse lattice spacing are shown in Figure 10. There is a considerable gap between the constituents of the multiplet, but further investigations are required to crosscheck the chiral extrapolations.

With the current results we are already able to make the first estimations of the scaling towards the continuum limit. The results in units of the scales $w_0^{0.2}$ and r_0 for the gluino-glue are shown in Figure 11. As expected, the results at $\beta = 5.8$ are unreliable. From the other lattice spacings a trend towards smaller gluino-glue masses is seen in the continuum limit.

The preliminary results of the extrapolations at different β in units of the scale $w_0^{0.2}$ are

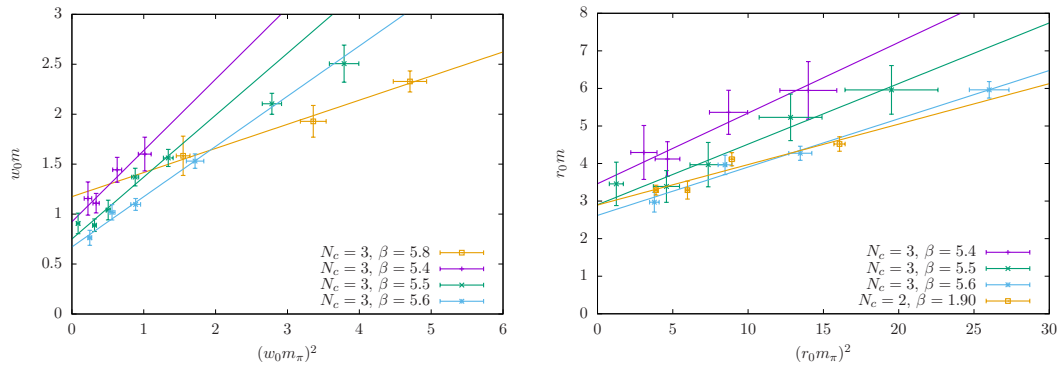

(a) scaling with $w_0^{0.2}$

(b) scaling with r_0

Figure 11: A comparison of the gluino-glue mass in units of the Sommer scale r_0 and of $w_0^{0.2}$ for different lattice spacings (corresponding to different β) and SU(N_c) gauge groups as a function of the squared adjoint pion mass. The simulations of SU(3) SYM at $\beta = 5.4$, 5.5, 5.6, and 5.8 have been done with a clover improved fermion action and a plain Wilson gauge action; the simulations of SU(2) SYM at $\beta = 1.9$ with a plain Wilson fermion action, one level of stout smearing, and a tree level Symanzik improved gauge action.

β	gluino-glue	glueball 0^{++}
5.4	0.90(13)	0.6240(59)
5.5	0.743(77)	0.84(20)
5.6	0.673(66)	0.60(15)

The masses in units of r_0 can be compared to our previous results for SU(2) SYM as shown in Figure 11. It is remarkable that the masses of the lightest states in physical units are comparable for SU(2) and SU(3) SYM.

8. Conclusions

Our current results for the lightest bound states in supersymmetric SU(3) Yang-Mills theory on the lattice already provide strong indications for a supermultiplet formation in the chiral continuum limit. As in the case of gauge group SU(2), there is no unexpected signature for supersymmetry breaking, and the lattice artefacts can be controlled. The non-perturbative numerical investigation of this theory with Wilson fermions is hence possible and the theoretical suggestions of Veneziano and Curci can be applied in practice.

The simulation parameters are quite restricted, since an SU(3) Yang-Mills theory with fermions in the adjoint representation demands considerably more computational efforts than in the case of the fundamental representation. The implementation of an improved fermion action is hence quite essential, as shown by our numerical results.

Further studies at larger lattices are required to complete the continuum extrapolation

and reduce finite volume uncertainties. Nevertheless, the present data already indicate that the multiplet formation persists towards the continuum limit. We are currently also exploring more advanced methods to reduce the excited state contamination from the determination of the masses of the bound spectrum.

9. Acknowledgements

The authors gratefully acknowledge the Gauss Centre for Supercomputing e. V. (www.gauss-centre.eu) for funding this project by providing computing time on the GCS Supercomputer JUQUEEN and JURECA at Jülich Supercomputing Centre (JSC) and SuperMUC at Leibniz Supercomputing Centre (LRZ). Further computing time has been provided on the compute cluster PALMA of the University of Münster. This work is supported by the Deutsche Forschungsgemeinschaft (DFG) through the Research Training Group "GRK 2149: Strong and Weak Interactions - from Hadrons to Dark Matter". G.B. acknowledges support from the Deutsche Forschungsgemeinschaft (DFG) Grant No. BE 5942/2-1.

References

[1] G. Bergner and S. Catterall, Int. J. Mod. Phys. A **31** (2016) 1643005 [arXiv: 1603.04478 [hep-lat]].

[2] G. Veneziano and S. Yankielowicz, Phys. Lett. B **113** (1982) 231.

[3] G. R. Farrar, G. Gabadadze and M. Schwetz, Phys. Rev. D **58** (1998) 015009 [arXiv: hep-th/9711166].

[4] G. R. Farrar, G. Gabadadze and M. Schwetz, Phys. Rev. D **60** (1999) 035002 [arXiv: hep-th/9806204].

[5] T. J. Hollowood, V. V. Khoze, W. J. Lee and M. P. Mattis, Nucl. Phys. B **570** (2000) 241 [arXiv: hep-th/9904116].

[6] G. Bergner, P. Giudice, I. Montvay, G. Münster and S. Piemonte, JHEP **1603** (2016) 080 [arXiv: 1512.07014 [hep-lat]].

[7] S. Ali, G. Bergner, H. Gerber, P. Giudice, S. Kuberski, I. Montvay, G. Münster and S. Piemonte, [arXiv: 1710.07464 [hep-lat]].

[8] A. Feo, R. Kirchner, S. Luckmann, I. Montvay and G. Münster, Nucl. Phys. Proc. Suppl. **83** (2000) 661 [arXiv: hep-lat/9909070].

[9] S. Ali, G. Bergner, H. Gerber, P. Giudice, I. Montvay, G. Münster and S. Piemonte, PoS(LATTICE2016) (2016) 222 [arXiv: 1610.10097 [hep-lat]].

[10] S. Ali, G. Bergner, H. Gerber, P. Giudice, S. Kuberski, I. Montvay, G. Münster and S. Piemonte, [arXiv: 1710.07105 [hep-lat]].

[11] M. Steinhauser, A. Sternbeck, B. Wellegehausen and A. Wipf, [arXiv: 1711.05086 [hep-lat]].

[12] G. Curci and G. Veneziano, Nucl. Phys. B **292** (1987) 555.

[13] D. Amati, K. Konishi, Y. Meurice, G. C. Rossi and G. Veneziano, Phys. Rept. **162** (1988) 169.

[14] S. Musberg, G. Münster and S. Piemonte, JHEP **1305** (2013) 143 [arXiv: 1304.5741 [hep-lat]].

[15] M. Lüscher, JHEP **1008** (2010) 071, Erratum: JHEP **1403** (2014) 092 [arXiv: 1006.4518 [hep-lat]].

[16] S. Borsanyi *et al.*, JHEP **1209** (2012) 010 [arXiv: 1203.4469 [hep-lat]].

[17] G. Bergner, P. Giudice, I. Montvay, G. Münster and S. Piemonte, Eur. Phys. J. Plus **130** (2015) 229 [arXiv: 1411.6995 [hep-lat]].

[18] G. Münster and H. Stüwe, JHEP **1405** (2014) 034 [arXiv: 1402.6616 [hep-th]].

[19] F. Farchioni, A. Feo, T. Galla, C. Gebert, R. Kirchner, I. Montvay, G. Münster and A. Vladikas, Eur. Phys. J. C **23** (2002) 719 [arXiv: hep-lat/0111008].

[20] S. Ali, G. Bergner, H. Gerber, I. Montvay, G. Münster, S. Piemonte and P. Scior, in preparation.

[21] S. Ali, G. Bergner, H. Gerber, P. Giudice, I. Montvay, G. Münster, S. Piemonte and P. Scior, [arXiv: 1711.05504 [hep-lat]].

[22] S. Ali, G. Bergner, H. Gerber, I. Montvay, G. Münster, S. Piemonte and P. Scior, in preparation.

[23] G. Bergner, I. Montvay, G. Münster, U. D. Özugurel and D. Sandbrink, PoS(Lattice 2011) 055 [arXiv: 1111.3012 [hep-lat]].

[24] H. Fukaya *et al.* [JLQCD Collaboration], Phys. Rev. D **92** (2015) 111501 [arXiv: 1509.00944 [hep-lat]].

[25] G. Bergner and J. Wuilloud, Comput. Phys. Commun. **183** (2012) 299 [arXiv: 1104.1363 [hep-lat]].

[26] G. Bergner, T. Berheide, I. Montvay, G. Münster, U. D. Özugurel and D. Sandbrink, JHEP **1209** (2012) 108 [arXiv: 1206.2341 [hep-lat]].

A. Data

In the following we list the data of our most relevant ensembles. The main part of the paper considers the runs on a $16^3 \times 32$ lattice at $\beta = 5.5$ with a one-loop clover coefficient $c_{sw} = 1.598$. These are summarised in the following table:

κ	am_π	r_0/a	am_{gg}	am_{gpp}	am_η	am_{f_0}	$am_{f_0,\mathrm{top}}$	N_{configs}
0.1637	0.9202(49)	3.86(11)	1.185(62)	0.63(13)	–	–	0.900(90)	500
0.1649	0.7888(19)	4.39(16)	0.995(28)	0.619(53)	0.76(11)	0.81(22)	0.680(80)	3212
0.1667	0.5475(19)	5.56(13)	0.739(24)	0.576(78)	0.620(35)	0.68(17)	0.580(80)	4415
0.1673	0.4437(26)	6.15(16)	0.648(28)	0.429(21)	0.582(31)	0.537(67)	0.550(80)	5984
0.1678	0.3360(23)	6.88(33)	0.492(36)	0.460(49)	0.439(75)	0.544(79)	–	3591
0.168	0.2651(51)	8.31(40)	0.420(21)	0.439(72)	–	–	–	2673
0.1683	0.138(15)	8.96(50)	0.429(39)	–	–	–	–	1645

All the quantities are in units of the lattice spacing a. The summarised quantities are the Sommer parameter r_0/a and the masses of the a–π (am_π), the gluino-glue (am_{gg}), the 0^{++} glueball (am_{gpp}), the a–η' meson (am_η), and the a–f_0 meson (am_{f_0}). In addition there is an alternative measurement of the a–f_0 meson mass from the correlator of the topological charge density ($am_{f_0,\mathrm{top}}$). N_{configs} is the number of generated thermalised configurations. Currently not the complete statistic is used in all measurements.